JOURNAL OF OPTOELECTRONICS AND ADVANCED MATERIALS Vol. 12, No. 12, December 2010, p. 2386 - 2390

DC resistivity and magnetic parameters of Ni-Cr-Zn nanoferrites

A. MAHESH KUMAR*, M. CHAITANYA VARMA, GSVRK CHOUDARY[b], K. SRINIVASA RAO[c], K.H. RAO[a], G. GOPALAKRISHNA
Department of physics, GITAM University, Visakhapatnam 530045, India
[a]*Department of physics, Andhra University, Visakhapatnam 530003, India*
[b]*Department of physics, BVB Vivenkanda College, Sainikpuri, Sec'bad 500094, India*
[c]*Department of Physics, PBN College, Nidubrolu 522124, India*

With a view to extend the frequency of operation of the Ni-Zn ferrites towards high frequency applications, magnetization and dc resistivity of the ferrites have been studied as a part of the investigation. Less value of saturation magnetization and resistivity has been noticed over the basic Ni-Zn ferrite.

(Received November 2, 2010; accepted November 25, 2010)

Keywords: Magnetization, DC resistivity, Initial permeability

1. Introduction

Magnetic ferrite nanoparticles are currently very promising materials because of their unique properties which makes them attractive from the scientific perspective as well as technological significance. High electrical resistivity coupled with highest possible saturation magnetization requires in order making use ferrites for high frequency applications minimizing the losses. Sizeable improvement in these parameters has been reported [1] earlier synthesizing Ni-Zn ferrites in the form of nanoparticles. Chromium ions which usually occupy octahedral sites in the ferrite lattice have chosen for the current investigation as it has been exhibited noticeable modifications in magnetic and electrical properties in bulk ferrites. At nanoscale, large number of ultrafine grains with huge grain boundary area would enhance the electrical resistivity of ferrites to the maximum extent possible. Less coordination of surface atoms results in uncompensated surface spins tending to create broken exchange bonds [2] which play a dominating role in altering the magnetic properties of nanoparticles. In addition, cation redistribution in nanoscale ferrites is the novel phenomena which lead to modify both electrical and magnetic properties further. Hence, in keeping these points in view, chromium has been substituted in place of iron in $Ni_{0.65}Zn_{0.35}Fe_2O_4$ as an extension to our earlier investigation.

2. Experimental details

$Ni_{0.65}Zn_{0.35}Fe_{2-x}Cr_xO_4$ (x = 0.00 to 0.2 in steps of 0.04) nanoparticles have been processed through sol-gel synthesis and the preparation methodology has been described elsewhere [1]. Powder X-ray diffraction analysis of all the samples has been done using a calibrated Philips (PW-3710) X-ray diffractometer coupled with PW-1800 software using Cu K_α ($\lambda = 1.5406$ A^o) radiation. Vibration sample magnetometer 115 PAR- EG&G model has been used to carry out room temperature saturation magnetization measurements and Keithley electrometer 614 has been utilized to measure dc electrical resistivity. Curie temperature measurement has been carried by Soohoo method [3]. Inductance values were measured using HP4192A LF Impedance analyzer at the small voltage of 1mV at a frequency of 1 kHz, from which the initial permeability was calculated with the equation $\mu_i = \frac{L}{L_0}$ where $L_0 = 0.4606\, N^2 h \log\left(\frac{OD}{ID}\right)\, \mu H$ [4, 5] is the air core inductance and N is the number of turns. Temperature dependence of initial permeability was also measured within the temperature range 40-100^{o}C using the formula

$$\text{Temperature Factor, } TF = \frac{\Delta\mu_i}{\mu_i^2 \Delta T} = \frac{1}{\mu_i}\alpha .$$

Here $\alpha = \frac{\Delta\mu_i}{\mu_i \Delta T}$ is the temperature coefficient of permeability. DC resistivity and initial permeability measurements were not carried out for x = 0.20, as cracks occurred repeatedly in the pellets during heat treatment.

3. Results and discussion

X-ray diffraction patterns of all the samples confirmed the single phase spinel structure (figure1).

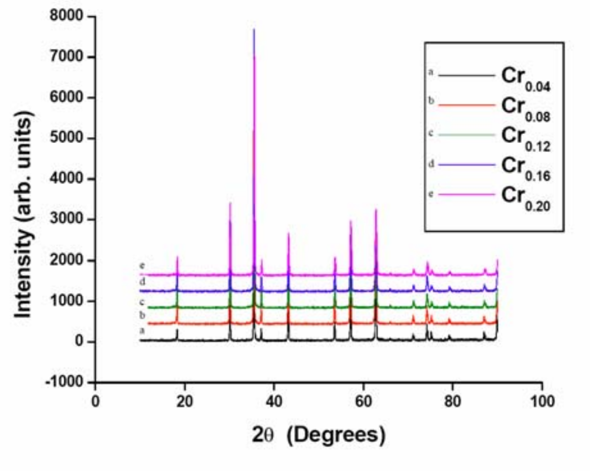

Fig. 1. X-ray diffraction pattern of $Ni_{0.65}Zn_{0.35}Fe_{2-x}Cr_xO_4$ *(x = 0.04 -0.20) annealed at 1080°C.*

Fig. 2 shows the lattice constant variation with increasing chromium concentration. Lattice constant '*a*' and Nelson-Riley function $F(\theta)=\frac{1}{2}\left(\frac{\cos^2\theta}{\sin\theta}+\frac{\cos^2\theta}{\theta}\right)$ [6] have been calculated for each peak of the X-ray pattern using diffraction angle θ and equation $a=d\sqrt{h^2+k^2+l^2}$. Nelson-Riley function indicates the error involved in the calculation of lattice constant. Accurate determination of lattice constant has been obtained from the extrapolation of calculated lattice constant against Nelson-Riley function for which the function is zero. The value of lattice constant for basic Ni-Zn ferrite has been found to be 8.3738 A° and coincides with that of the reported [7, 8].

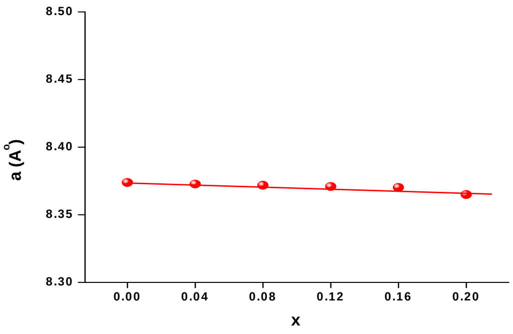

Fig. 2. Lattice constant as a function of chromium concentration.

Room temperature hysteresis loops of chromium substituted Ni-Zn ferrites are shown in figure. Ni-Zn basic composition has been exhibited the highest value of saturation magnetization ever reported [1]. The reasons for the observed highest value of saturation magnetization (80 emu/g) have been explained on the basis of core-shell model [9].

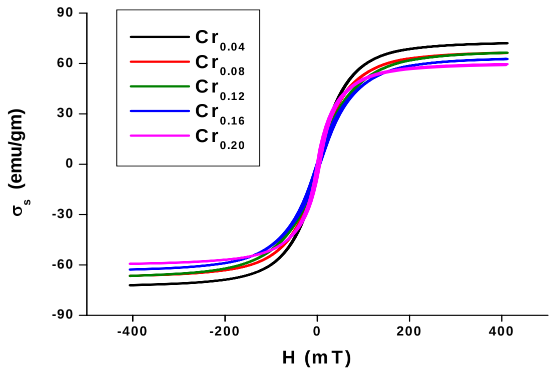

Fig. 3. Room temperature hysteresis loops of chromium substituted Ni-Zn ferrites.

Saturation magnetization decreases almost linearly with increasing chromium concentration. The site occupancy of indium ions in the spinel lattice can be envisaged on the basis of variations in the magnetization values. If the chromium ions enter the A-sublattice only, replacement of A-site Fe^{3+} ions by paramagnetic chromium ions lead to the dilution of the A-sublattice magnetic moment. The net magnetization of the sublattices, M_B-M_A, decreases so rapidly by weakening the superexchange interactions and a large fall in magnetization has to be expected. The fall in magnetization is rapid up to chromium concentration of 3 mol % and there after a slow decrease is clearly seen. Hence, the possibility of entering chromium ions into A-sites can be ruled out. If chromium ions enter B-sublattice only, replacement of B-site Fe^{3+} ions by chromium ions causes the dilution of B-sublattice magnetic moment. This dilution decreases the magnetic moment of the octahedral sublattice by weakening the A-B superexchange interaction. The saturation magnetization decreases gradually with increasing the concentration of chromium. Such a decrease in magnetization has been noticed up to a chromium content of 3 mole % and not much variation has seen for later concentrations. A slight deviation from linearity is saturation magnetization beyond 3 mole % is due to increased porosity supported from the density measurements. The strong preference of chromium ions towards octahedral sites has been mentioned in some earlier reports [10-12].

If chromium ions have their preference for both A and B sites in the spinel lattice, the replacement of both the tetrahedral and octahedral Fe^{3+} ions by chromium ions leads to cause much more weakening of the A-B exchange interactions. Then B-B interaction comes in to play and one expects a large reduction in saturation magnetization as described above. Measured Curie temperature values (discussed below) do not support the observed decrease in

Curie temperature values indicating that A-B interaction is still predominant. Hence, the possibility of chromium entering into B-sites can be taken into consideration on the basis of observed results as well as reported in the literature.

Linear decrease in Curie temperature has been noticed with increasing chromium concentration (figure). The observed variations in Curie temperature have been explained on the basis of the superexchange interactions among the tetrahedral and octahedral cations in the spinel lattice. As is known the net magnetic moment of the spinel lattice is the difference between the magnetic moments of the B and A sublattices. Hence, it is therefore expected that greater amount of thermal energy will be required to off-set the influence of exchange interactions. Paramagnetic chromium ions prefer to occupy [13] octahedral sites and decrease the density of magnetic ions at the B-sublattice leading to decrease in the Curie temperature.

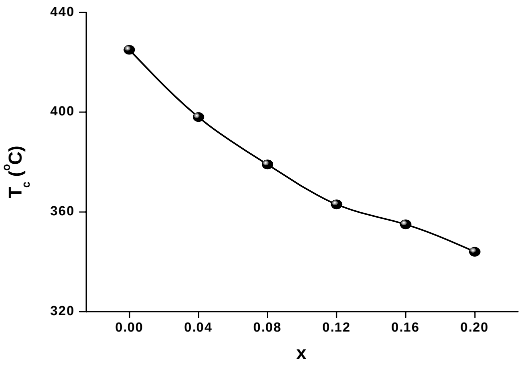

Fig. 4. Variation in Curie temperature as a function of chromium concentration.

With increasing chromium concentration, dc resistivity slightly decreases and increases further. DC resistivity measurement has not been carried out for x = 0.20, as cracks occurred repeatedly in the pellets during heat treatment. Chromium ions are known to have strong site preference for B-sites [12] in the spinel lattice which do not participate in the conduction mechanism but limit the degree of hopping among $Fe^{2+} \leftrightarrow Fe^{3+}$ pairs. An increase in resistivity is therefore expected with increasing chromium concentration. Similar increase in resistivity has been in the current study beyond 2 mol % of chromium. The ionic radius of chromium (0.61 A^o) noticed to be slightly than that of iron (0.65A^o).

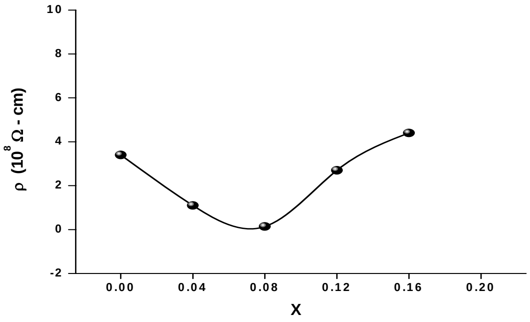

Fig. 5. Variation in resistivity as a function of concentration of chromium.

Replacement of iron with chromium at octahedral sites reduces the distance between the lattice sites which is evident from lattice constant measurements. The distance between the two metal ions in B-site is smaller than the distance between a metal ion at B-site and another metal ion at A-site. The electron hopping between A-B sites under normal conditions has therefore very small probability compared to that of B-B hopping. At initial concentrations, very few iron ions are replaced by chromium ions which may increase hopping probability by shrinking the lattice slightly. With increasing chromium, the number of iron ions becomes less and hence a decrease in hopping probability among $Fe^{2+} \leftrightarrow Fe^{3+}$ pairs leads to increase in resistivity.

Activation energies for all the samples have been determined from the slope of log of resistivity (log ρ) versus reciprocal of absolute temperature (1/T) plots and are given in tables 5.4 and 5.5.

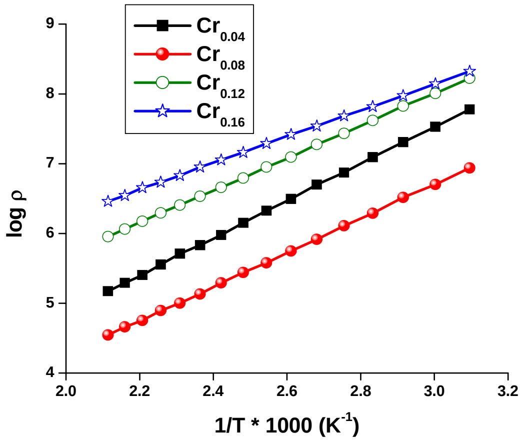

Fig. 6. Temperature dependence of resistivity of $Ni_{0.65}Zn_{0.35}Fe_{2-x}Cr_xO_4$ (x = 0.0 4 -0.16) for an applied field of 1 V/m.

Table 1: Activation energy values (in eV) of chromium substituted Ni-Zn ferrites.

X	0	0.04	0.08	0.12	0.16	0.20
E_A (eV)	0.50	0.53	0.48	0.46	0.37	-

The observed variation in activation energies are in accordance with the observed changes in the resistivity values of the samples. In general, in ferrites, the activation energy is decided by the hopping probability of electrons and holes among $Fe^{3+} \leftrightarrow Fe^{2+}$ and $Ni^{3+} \leftrightarrow Ni^{2+}$ pairs respectively. Activation energy required for conduction due to electron hopping in ferrites is found to be in the order of 0.4 eV [14]. Still much energies are needed for hole hopping compared to electron hopping. Higher values of activation energies (> 0.4 eV) have been noticed for all the samples in the present study. These activation energy values suggest that the hopping of both the charge carriers (electrons and holes) is responsible for electrical conduction in all the ferrite samples. Similar inferences regarding the higher activation energies have been reported [15-17] by some researchers.

A steep fall in initial permeability has been noticed for initial concentrations of chromium and at higher concentrations it found to be independent of impurity concentration.

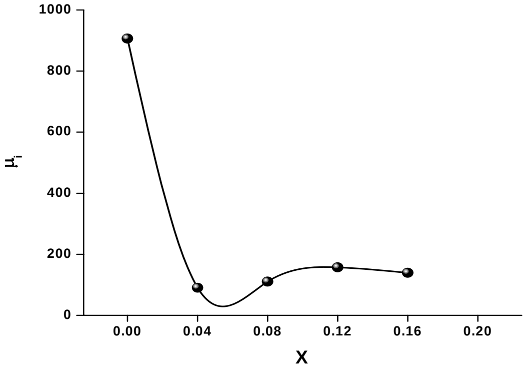

Fig. 7. Variation in initial permeability as a function of concentration of chromium ion.

Highest value of initial permeability (900) has been found in $Ni_{0.65}Zn_{0.35}Fe_2O_4$ which might be reasonably higher value when compared to available values in the literature [18-22] in Ni-Zn ferrite system. As the initial permeability is directly proportional to the saturation magnetization [23] of the material, the observed high value of initial permeability might be possible because of the highest saturation magnetization (80 emu/g) recorded in the sample.

Though initial permeability is sensitive to many parameters as describe above, the variations in the initial permeability in the present investigation have been explained by taking grain size into consideration. Initial permeability is connected to grain size as

$$\mu \propto D^{1/3}$$

where D is the grain diameter.

In chromium Ni-Zn ferrites, fine grains have been observed for initial concentrations (x = 0.04 and 0.08) and bigger grains with segregation of some material phases at higher concentrations. The precipitation of extra phases in the material hinders the domain wall motion and thereby decreasing the initial permeability. The decrease in initial permeability with increasing concentration of chromium has also been attributed to the decrease in density. Temperature factor of initial permeability and temperature dependence of initial permeability (40°C and 100°C) as a function of in all the samples is shown in figures.

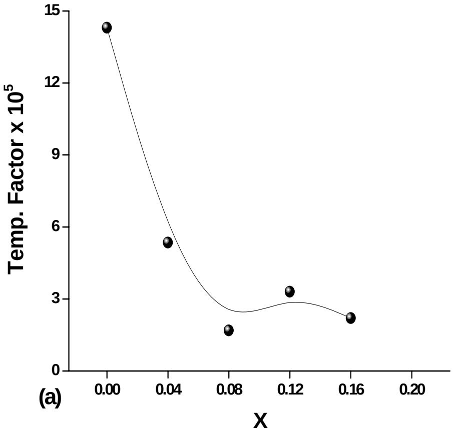

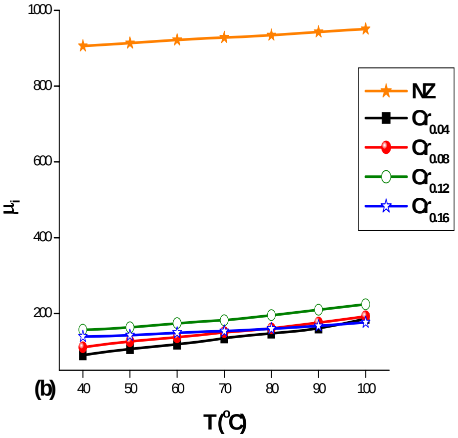

Fig. 8. (a) Temperature factor of initial permeability (b) Temperature dependence of initial permeability for chromium substituted Ni-Zn ferrites.

The parameters initial permeability and the temperature factor of initial permeability have been observed to follow the same trend with increasing chromium concentration. Temperature dependence of initial permeability in any sample is found to increase steadily within the temperature range 40-100°C indicating these toroids can be operated efficiently above 100°C which is higher than the earlier reported value (80°C) [24].

References

[1] A. Mahesh Kumar, M. Chaitanya Varma, Charu Lata Dubey, K. H. Rao, S. C Kashyap J. Magn. Magn. Mater. **320**, 1995 (2008).

[2] R. N. Bhowmik, R. Ranganathan Solid State Commun. **141**, 365(2007).

[3] R. F. Soohoo, Theory and Applications of Ferrites Englewood Cliffs, NJ: Printice-Hall (1960) p. 24.

[4] A. Lakshman, K. H. Rao, R. G. Mendiratta J. Magn. Magn. Mater. **250**, 92 (2002).

[5] K. H. Rao, N. K. Gaur, K. Aggarwal, R. G. Mendiratta J. Appl. Phys. **53**, 1122(1982).

[6] B. D. Cullity, S. R. Stock “Elements of X-ray diffraction”, third Ed. Prentice-Hall Inc. New Jersey (2001) p.388.

[7] J. M. Daniels, A. Rosenwaig Can. J. Phys. **48**, 381 (1970).

[8] L. K. Leung, B. J. Evans, A. H. Morrish Phys. Rev. B **8**, 29 (1973).

[9] A. Mahesh Kumar, K. H. Rao, J. M. Greneche J. Appl. Phys. **105**, 073919 (2009).

[10] R. Laishram, S. Phanjoubam, H. N. K. Sarma, Chandra Prakash J. Phys. D: Appl. Phys. **32**, 2151 (1999).

[11] K. P. Chae, Y. B. Lee, J. G. Lee, S. H. Lee J. Magn. Magn. Mater. **220**, 59 (2000).

[12] S. H. Lee, S. J. Yoon, G. J. Lee, H. S. Kim, C. H. Yo, K. Ahn, D. H. Lee, K. H. Kim Mater. Chem. Phys. **61**, 147 (1999).

[13] K. P. Chae, Y. B. Lee, J. G. Lee, S. H. Lee J. Magn. Magn. Mater. **220**, 59 (2000).

[14] A. M. Abdeen, J. Magn. Magn. Mater. **192**, 121 (1999).

[15] C. N. Chinnasamy, A. Narayanasamy, N. Ponpandian, K. Chattopadhyay, K. Shinoda, B. Jayadevan, K. Tohji, K. Nakatsuka, T. Furubyashi, I. Nakatani Phys. Rev. B **63**, 184108 (2001).

[16] N. Ponpandian, P. Balaya, A. Narayanasamy J. Phys: Condens. Matter. **14**, 3221 (2002).

[17] A. Verma, O. P. Thakur, C. Prakash, T. C. Goel, R. G. Mendiratta Mater. Sci.& Engg. B **116**, 1 (2005).

[18] H. Su, H. Zhang, X. Tang, Y. Jing, Y. Liu J. Magn. Magn. Mater. **310**, 17 (2007).

[19] A. Verma, T. C. Goel, R. G. Mendiratta J. Magn. Magn. Mater. **210**, 274 (2000).

[20] S. Zahi, M. Hashim, A. R. Daud, J. Magn. Magn. Mater. **308**, 177 (2007).

[21] D. Condurache, C. Pasnicu, E. Luca “International Conference on Ferrites”, ICF – **4,** 157 (1985).

[22] R. V. Mangalaraja, S. Thomas Lee, S. Ananthakumar, P. Manohar, Carlos P. Camurri Mater. Sci. Eng. A **476**, 234 (2008).

[23] J. Smit, H. P. J. Wijn “Ferrites” Philips Technical Library, Eindhoven (1959) 244.

[24] B. P. Rao, K. H. Rao J. Magn. Soc. Jpn. **22**, 305 (1998).

---

[*] Corresponding author: drmaheshnano@gmail.com